Magnetic Field Gradients in Solid State Magic Angle Spinning NMR

W. E. Maas,* A. Bielecki,* M. Ziliox,* F. H. Laukien,* and D. G. Cory†,[1]

*Bruker Instruments, Inc., 44 Manning Road, Billerica, Massachusetts 01821; and †Department of Nuclear Engineering, Massachusetts Institute of Technology, Cambridge, Massachusetts 02139

Magnetic field gradients have proven useful in NMR for coherence pathway selection, diffusion studies, and imaging. Recently they have been combined with magic angle spinning to permit high-resolution measurements of semi-solids, where magic angle spinning averages any residual dipolar couplings and local variations in the bulk magnetic susceptibility. Here we show the first examples of coherence pathway selection by gradients in dipolar coupled solids. When the gradient evolution competes with dipolar evolution the experiment design must take into account both the strength of the dipolar couplings and the means to refocus it. Examples of both homonuclear and heteronuclear experiments are shown in which gradients have been used to eliminate the need for phase cycling. © 1999 Academic Press

Gradient enhanced NMR spectroscopy is widely used in liquid state spectroscopy for coherence pathway selection, solvent suppression, artifact reduction, and diffusion weighting and has had a tremendous impact by improving the quality of NMR spectra (*1–4*). To date, the same advantages have not been realized in high-resolution solid state NMR. The requirements in solid state spectroscopy are of course different; rarely does one encounter a solvent-like signal (so limited dynamic range is rarely a consideration) and typically the number of scans is sufficient to permit extensive phase cycling. The applications of magnetic field gradients in solid state NMR will be to vary the spin dynamics and to eliminate artifacts, especially in two-dimensional spectra.

An important difference between liquid and solid state studies is the change in geometry associated with magic angle sample spinning (MAS). For high-resolution solid state NMR spectroscopy, magic angle spinning is nearly always used to reduce the second-rank tensorial interactions to their isotropic average. This is particularly important for chemical shift interactions, which otherwise cause extensive spectral overlap. Since the sample is spinning rapidly, typically 5 to 20 kHz, around an axis oriented at the magic angle ($\theta_m = \cos^{-1}(1/\sqrt{3})$), the commonly used gradient field geometry $\partial B_z/\partial z$ introduces a gradient interaction which is dependent on the sample geometry, the spinner rotation, and the specific experiment performed. The correct approach is to introduce a gradient interaction that is not temporally modulated by the sample spinning. Such a gradient is oriented along the magic angle axis, $\partial B_z/\partial \theta_m$, and has been described (*5*).

To date, MAS and gradients have been combined in high-resolution MAS studies of semi-solid samples (*5*), MAS diffusion studies (*6*), imaging (*7, 8*), and solid state NMR (*9, 10*). In high-resolution MAS (hr-MAS) studies, magic angle spinning is used to increase the spectral resolution of nonsolid samples which, in the nonspinning case, exhibit line broadening due to residual dipole–dipole couplings and magnetic susceptibility variations. Gradients are used for coherence pathway selection, solvent suppression, and artifact reduction. Hr-MAS has found applications in combinatorial chemistry, studies of excised tissue and cultured cells, and studies of lipids (*5, 11–16*). In heterogeneous samples, variations in the magnetic susceptibility over the sample lead to line broadening and background gradients. MAS averages the susceptibility-induced background gradients, and the combination of MAS and gradients enables correct diffusion measurements to be made in these complex samples (*6*). Applications include diffusion in granular media, porous materials, and biological tissue. In solid state imaging, MAS is used to lengthen the effective T_2, which results in a better image resolution. The elimination of susceptibility broadening leads to distortion-free images. MAS also permits image contrast to be based on the isotropic chemical shift (*7, 8*).

The application of a magnetic field gradient creates a spatial modulation across the sample. This modulation or grating (*17*) can be used to suppress a resonance or to selectively refocus signals based on a specific coherence pathway. The challenge in solids is to create a grating without destroying the magnetization, i.e., the time required to burn a grating should be short compared to the decoherence time of the transverse coherences.

The task of creating a magnetization grating in dipolar-coupled solid samples on a time scale smaller than the effective relaxation time has been widely explored in solid state imaging. The conclusions from imaging studies are relevant to the application of gradients in solid state NMR and show that gradient experiments must be tailored to the spin dynamics of
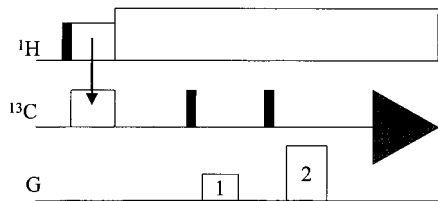
FIG. 1. In the double-quantum filtered experiment, carbon magnetization is generated via cross polarization from protons and this magnetization subsequently evolves under the homonuclear dipolar coupling into an antiphase state. This state is transferred to a double-quantum state and dephased by a first magnetic field gradient pulse. A second gradient pulse is given after the state has been transferred back to a single-quantum state. When the amplitude of this second gradient pulse is twice that of the first one, only magnetization that went through a double-quantum state will be refocused.

the sample under study (*18*). Three classes of gradient experiments can be distinguished as follows.

1. Motionally reduced dipole–dipole couplings. MAS averages the residual dipolar interactions and any background gradients from local variations in the bulk susceptibility. Gradient methods that are typical of liquid state approaches suffice (*9*).

2. Heteronuclear and weak homonuclear couplings. Strong RF fields are applied for heteronuclear decoupling, while weaker couplings between the dilute nuclei are averaged by MAS. The gradient methods are similar to those used in liquid state experiments, but care has to be taken with the variation of the decoupling efficiency under the gradient-induced offset. Strong RF fields and relatively weak gradients are applied.

3. Homonuclear experiments (strong coupling). Here coherent averaging schemes (multiple-pulse or magic echoes) must be used to reduce the homonuclear dipolar couplings. Since the gradient interaction will not commute with the dipolar Hamiltonian in the toggling frame, the gradient pulses are inserted in selected windows of coherent averaging schemes. The gradients should therefore be applied as short, strong pulses (*19*).

A separate case involves the study of quadrupolar nuclei, in which dipolar couplings are usually not an issue. Fast MAS is used here to increase the effective T_2, and decoupling is usually not needed. Coherence selection in MQMAS experiments can be performed with short, strong gradient pulses (*10*).

In this paper, we present the results from three different solid state NMR experiments. These examples illustrate the issues involved with the last two categories listed above. All experiments were obtained on Bruker Avance spectrometers, operating at proton frequencies of 400 and 500 MHz, using CP-MAS probes with 4-mm-od rotors and equipped with magic angle gradients (5.5×10^{-2} Tm^{-1} A^{-1}).

An example of a homonuclear experiment with weak dipolar couplings is a carbon double-quantum filter (Fig. 1). The results from a sample of doubly ^{13}C-labeled glycine are depicted in Fig. 2. In this case, fast MAS averages the dipolar interaction between the dilute nuclei, which may be reintroduced by rotational resonance, in which the MAS rotation

speed is matched to the separation of the resonance lines of the coupled nuclei (*20–22*). This selective recoupling provides for coherence transfers that occur via both double- and zero-quantum coherence pathways. A gradient-enhanced double-quantum filtered experiment restricts the transfer to only the double-quantum pathway (*23*).

In the above experiment, the rotational resonance condition reintroduces the dipolar coupling between the carbon spins. Evolution under this Hamiltonian creates an antiphase state that is transferred to a double-quantum state by a RF pulse. The applied magnetic field gradient induces a spatially dependent phase shift, proportional to the coherence order of the spin state. Integration of the magnetization over the sample results in zero net magnetization, hence the term dephasing. A second gradient pulse, given after the state has been transferred back to a single quantum state, refocuses that part of the magnetization that evolved as a +2 quantum coherence. Double-quantum filtering is achieved by a 1:2 ratio of the amplitudes of the
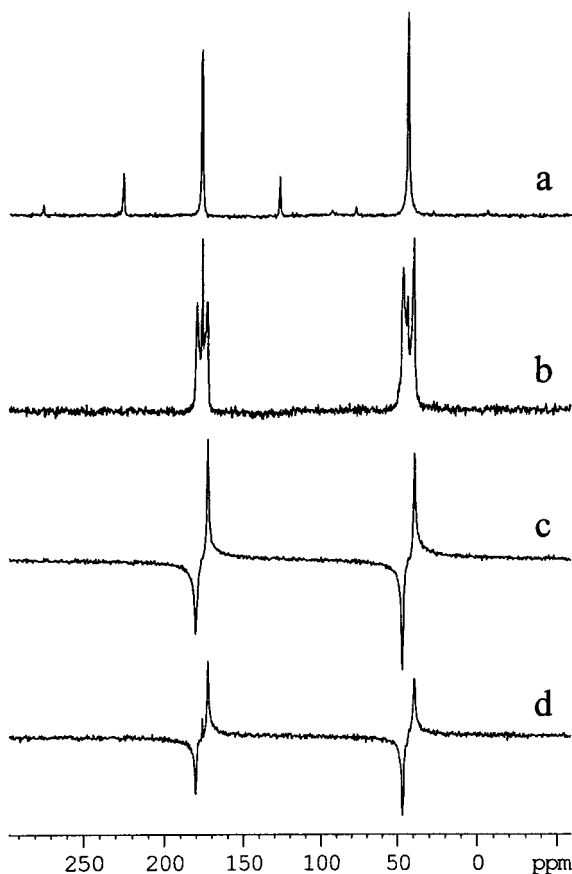

FIG. 2. Carbon spectra of doubly labeled glycine, obtained at a magnetic field strength of 9.4 T (400 MHz). The top two spectra are obtained off (a) and on (b) the rotational resonance condition, respectively. The lower spectra are double-quantum-filtered spectra, with coherence selection obtained via phase cycling (c) and with magnetic field gradients (d). The dipolar evolution time was 1 ms; gradient pulses were 250 μs at a strength of 20 and 40 G/cm, respectively. Sixteen scans were accumulated for the double-quantum-filtered experiments.
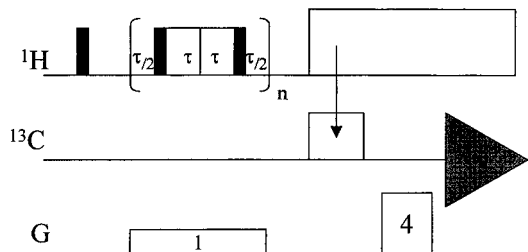
FIG. 3. A magic echo cycle is used to refocus the homonuclear dipolar interaction, while a simultaneously applied magnetic field gradient creates a grating on the proton spin. Spin-locking the proton magnetization converts this grating to an amplitude-modulated cosine grating, which retains half of the initial proton reservoir. This amplitude-modulated grating is transferred to ^{13}C and then refocused by a second gradient. The gradients are applied at a 1 to 4 ratio, according to the gyromagnetic constants of protons and carbons.

gradient pulses. The expected double-quantum spectrum is in an antiphase state.

The transfer efficiency in rotational resonance can be used to measure the distance (via the dipolar coupling strength) between the selected spins. An advantage of restricting the pathways over which a coherence is transferred is that the distance calibration is simplified if the transfer is isolated to either the double-quantum or the zero-quantum pathway (23). There are, however, two costs associated with using gradients in this experiment. First, for the sequence as written, the gradient selects only the $+2$ quantum pathway and therefore half of the potential signal (that which went through the -2 state) is lost. In addition, the system is forced to evolve for a finite time in the double-quantum state, and this state decays more quickly than the single quantum. This time is longer than would be necessary in a phase-cycled measurement, where the only time required is that to change the RF phase.

In the next example, we demonstrate that a magnetization grating can be created in a spin system with strong dipolar couplings. The challenge in such a system is to create a grating in a short time compared to the lifetime of the transverse magnetization. Since in a typical rigid solid, the proton T_2^* is on the order of only tens of microseconds, coherent averaging techniques need to be employed in combination with magnetic field gradients (18, 19).

In this experiment (Figs. 3 and 4), a sequence of magic echo cycles is used to lengthen the proton decay time. A magic echo cycle refocuses the homonuclear dipolar interaction (24, 25) and provides a convenient window in which to place the gradient. After generation of proton magnetization and a series of magic echoes concurrent with a magnetic field gradient, a grating is created on the proton spins, $k = \gamma_H \int G(\tau)d\tau$. The spatial grating can be envisioned as the proton magnetization wound in a helix along the spinner axis.

The use of gradients in heteronuclear studies depends on the efficient transfer of the grating to a heteronucleus. Such a transfer can be achieved simply through cross polarization. A spin-locking RF pulse applied to the proton system locks only

those magnetization components parallel to the applied RF field. The spatially phase-modulated grating is hence converted to an amplitude-modulated cosine grating, with a loss of half of the proton reservoir (26). This amplitude-modulated grating is transferred to ^{13}C and then refocused by a second gradient of four times the amplitude. The factor of 4 arises from the ratio of the gyromagnetic ratios of proton and carbon spins; the grating on carbon unwinds four times slower than the creation of a grating on protons.

The experiment can be thought of as a gradient-filtered cross-polarization in which the gradients replace spin temperature alternation as a means of suppressing the Zeeman polarized signal. Figure 4 shows the results of this experiment on a sample of glycine. While there is little need for gradient selection to limit the pathways in cross-polarization measurements, the above sequence opens the way for gradient-based spectral editing.

The third example of using gradients in solid state MAS NMR is a heteronuclear experiment in which two weakly coupled nuclei are correlated. In heteronuclear correlation experiments, gradients may be used to suppress the magnetization of the uncorrelated spins through the formation of a heteronuclear gradient echo. Since the signals from the correlated spins are usually much smaller than those from uncoupled spins, the use of gradients presents a clear advantage. In the gradient version of the experiment, coherence selection is achieved in each individual scan, eliminating the need to use phase cycling to subtract the large signals of the uncoupled spins.
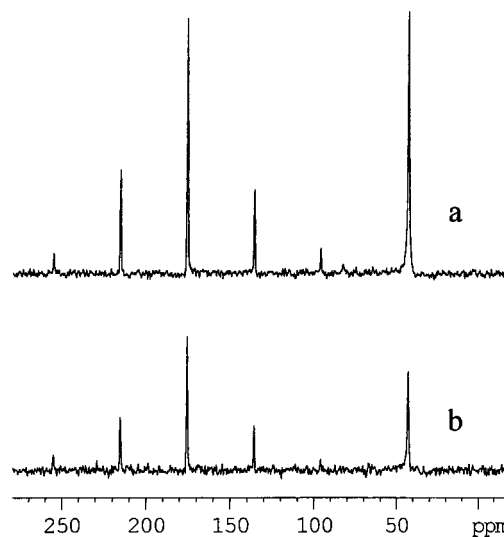

FIG. 4. Carbon spectra of natural abundance glycine, obtained at a magnetic field strength of 9.4 T (400 MHz). The top spectrum is obtained by transferring magnetization from protons to carbons after the proton dipolar couplings have been refocused by a series of magic echo sequences. In the lower spectrum, a gradient is used to impose a grating on the protons prior to transferring the magnetization to carbon. The magic echo time τ was 25 μs and four cycles were applied. Gradients of 10 and 40 G/cm were used, respectively.
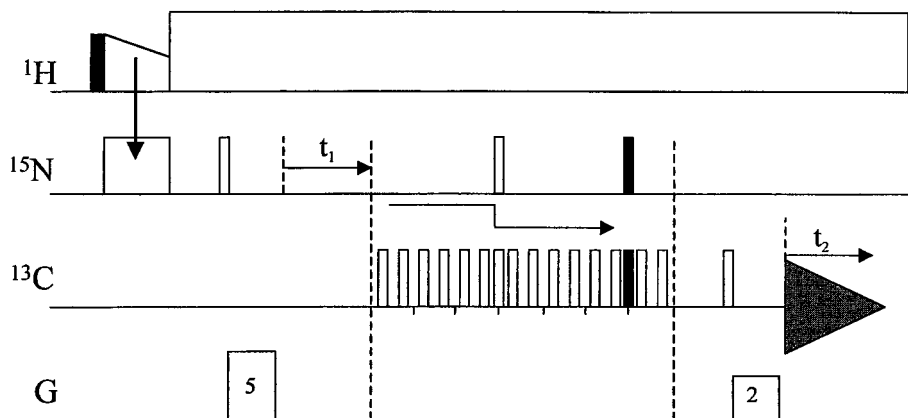
FIG. 5. Pulse sequence of the 2D gradient-enhanced heteronuclear correlation sequence. Nitrogen magnetization is first created by cross polarization from protons. A magnetization grating is then created on the nitrogen spins. A TEDOR sequence transfers the magnetization grating to carbon and after reconversion to in-phase carbon magnetization the grating is refocused by a second gradient pulse. (The filled bars represent 90° pulses, while the open bars represent 180°). The ratio of the gradient strengths reflects the ratio of the gyromagnetic constants of nitrogen and carbon. The sequence differs from a conventional correlation experiment by the addition of two free evolution periods in which the gradient pulses are placed.

The example shown in Fig. 5 is a two-dimensional nitrogen–carbon correlation. Nitrogen magnetization is generated from cross polarization from protons and is transferred, after evolution during t_1, to carbons. In this particular experiment, a transferred echo double resonance or TEDOR (27) sequence is used to correlate the nitrogen spins to dipolar coupled carbon spins. (Alternatively, the nitrogen magnetization can be transferred to carbon via a ramped CP sequence.) A grating is created on the nitrogen prior to the transfer and refocused after the creation of in-phase carbon magnetization. The ratio of the amplitudes of the gradient pulses is adjusted according to the ratio of the gyromagnetic constants of the heteronuclei.

Figure 6 shows the result of this experiment on a sample of uniformly ^{13}C- and ^{15}N-labeled arginine. Additional free evolution periods, equal to multiples of the rotor period, have been used both before and after the TEDOR transfer. These periods provide windows in which to place the gradient pulses. The use of π pulses refocuses the chemical shift evolution during these periods. Note that when using shorter and stronger gradient pulses, these can be inserted in the TEDOR sequence itself, eliminating the need for these additional periods. The experiment was performed with 200-μs gradient pulses of 55 and 22 G/cm, respectively. The use of magnetic field gradients introduces a spatially dependent offset across the sample, which interferes with the efficiency of the proton decoupling during the gradient intervals.

Magnetic field gradients can be introduced in solid state NMR experiments, provided that the experiment is designed to take into account the strength of the dipolar couplings. In this paper, three experiments are shown, illustrating the case of weak homonuclear, strong homonuclear, and heteronuclear dipolar couplings. We show that gradients can be useful even in the presence of dipolar coupling, employing coherence selection via the dipolar coupling, as well as together with heteronuclear dipolar decoupling. The loss of

signal associated with the use of gradients in these experiments compared to their phase-cycled versions can be tolerated, provided that the advantages of improved spectral quality and cleaner coherence selection are realized. We expect that the use of gradients in solid state MAS spectroscopy will find useful applications.
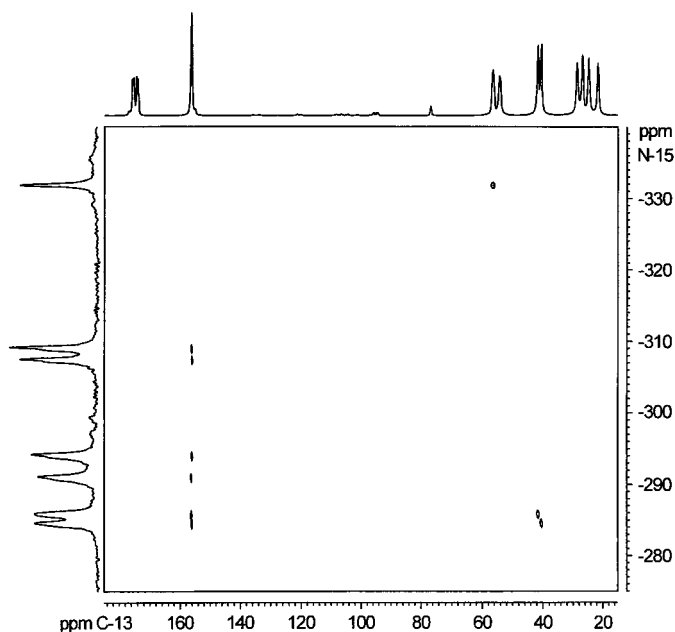

FIG. 6. Two-dimensional nitrogen–carbon correlation spectrum of uniformly ^{13}C- and ^{15}N-labeled arginine, obtained at a magnetic field strength of 11.7 T (500 MHz). The spectrum is obtained via magnetization transfer from nitrogen to carbon. The sample was spun at 10 kHz, and the dipolar evolution times equaled three rotor cycles. Gradient pulses of 55 and 22 G/cm were used on ^{15}N and ^{13}C, respectively, for a duration of 200 μs. Two scans were accumulated per fid, and 2 fids were acquired for each of the 128 t_1 increments (States method).

REFERENCES

1. R. E. Hurd, Gradient-enhanced spectroscopy, *J. Magn. Reson.* **87,** 422–428 (1990).

2. P. C. M. v. Zijl and C. T. Moonen, Complete water suppression for solutions of large molecules based on diffusional differences between solute and solvent (DRYCLEAN), *J. Magn. Reson.* **87,** 18 (1990).

3. M. Piotto, V. Saudek, and V. Sklenar, Gradient tailored excitation for single-quantum NMR spectroscopy of H2O solutions, *J. Biomol. NMR* **2,** 661 (1992).

4. W. S. Price, Gradient NMR, *Ann. Rep. NMR* (1995).

5. W. E. Maas, F. H. Laukien, and D. G. Cory, Gradient, high resolution, magic angle sample spinning NMR, *J. Am. Chem. Soc.* **118,** 13085 (1996).

6. X.-W. Tang, personal communication.

7. R. Wind and C. S. Yannoni, U.S. Patent 4 301 410 (1981).

8. D. G. Cory, J. W. M. v. Os, and W. S. Veeman, MAS imaging, *J. Magn. Reson.* **76,** 543 (1989).

9. T. Fritzhanns, S. Hafner, D. E. Demco, H. W. Spiess, and F. H. Laukien, Pulsed field gradient selection in two-dimensional magic angle spinning NMR spectroscopy of dipolar solids, *J. Magn. Reson.* **134,** 355 (1998).

10. C. A. Fyfe, J. Skibsted, H. Grondey, and H. Meyer, Pulsed field gradient multiple quantum MAS NMR spectroscopy of half-integer spin quadrupolar nuclei, *Chem. Phys. Lett.* **281,** 44 (1998).

11. J. D. Gross, P. R. Costa, J.-P. Dubacq, D. E. Warschawski, P.-N. Lirsac, P. F. Devaux, and R. G. Griffin, Multidimensional NMR in lipid systems. Coherence transfer through J couplings under MAS, *J. Magn. Reson. B* **106,** 187 (1995).

12. K. K. Millis, W. E. Maas, D. G. Cory, and S. Singer, Gradient, high-resolution, magic angle spinning nuclear magnetic resonance spectroscopy of human adipocyte tissue, *Magn. Reson. Med.* **38,** 399 (1997).

13. L. L. Cheng, M. J. Ma, L. Becerra, T. Ptak, I. Tracey, A. Lackner, and R. G. Gonzalez, Quantitative neuropathology by high resolution magic angle spinning proton magnetic resonance spectroscopy, *Proc. Natl. Acad. Sci. USA* **94,** 6408 (1997).

14. R. C. Anderson, M. A. Jarema, M. J. Shapiro, J. P. Stokes, and M. Ziliox, NMR techniques in combinatorial chemistry, *J. Org. Chem.* **60,** 2650 (1995).

15. L. L. Cheng, C. L. Lean, A. Bogdanova, S. C. Wright, J. L. Ackerman, T. J. Brady, and L. Garrido, Enhanced resolution of proton NMR spectra of malignant lymph nodes using magic-angle spinning, *Magn. Reson. Med.* **36,** 653 (1996).

16. S. K. Sarkar, R. S. Garigipati, J. L. Adams, and P. A. Keifer, An NMR method to identify nondestructively chemical compounds bound to a single solid-phase-synthesis bead for combinatorial chemistry applications, *J. Am. Chem. Soc.* **118,** 2305 (1996).

17. T. R. Saarinen and J. C. S. Johnson, Imaging of transient magnetization gratings in NMR. Analogies with laser-induced grating and application to diffusion and flow, *J. Magn. Reson* **78,** 257 (1988).

18. D. G. Cory, J. B. Miller, R. Turner, and A. N. Garroway, Multiple-pulse methods of ¹H NMR imaging of solids: second-averaging, *Mol. Phys.* **70,** 331 (1990).

19. J. B. Miller, D. G. Cory, and A. N. Garroway, Pulsed field gradient NMR imaging of solids, *Chem. Phys. Lett.* **164,** 1 (1989).

20. D. P. Raleigh, M. H. Levitt, and R. G. Griffin, Rotational resonance in solid state NMR, *Chem. Phys. Lett.* **146,** 71 (1988).

21. M. G. Colombo, B. H. Meier, and R. R. Ernst, Rotor-driven spin diffusion in natural abundance ¹³C spin systems, *Chem. Phys. Lett.* **146,** 189 (1988).

22. W. E. Maas and W. S. Veeman, Natural abundance ¹³C spin diffusion enhanced by magic angle spinning, *Chem. Phys. Lett.* **149,** 170 (1988).

23. N. C. Nielsen, F. Creuzet, R. G. Griffin, and M. H. Levitt, Enhanced double-quantum nuclear magnetic resonance in spinning solids at rotational resonance, *J. Chem. Phys.* **96,** 5668 (1992).

24. S. Matsui, *Chem. Phys. Lett.* **179,** 187 (1991).

25. S. Hafner, D. Demco, and R. Kimmich, *Solid State NMR* **6,** 275 (1996).

26. A. Sodickson and D. G. Cory, A generalized k-space formalism for treating the spatial aspects of a variety of NMR experiments, *Prog. NMR Spectrosc.* **33,** 77 (1998).

27. A. W. Hing, S. Vega, and J. Schaeffer, Transferred-echo double-resonance NMR, *J. Magn. Reson.* **96,** 205 (1992).